

# Platinum(II) Co-ordination Chemistry of Bis(diphenylphosphino)amine†

C. Scott Browning and David H. Farrar\*

Department of Chemistry, University of Toronto, Toronto, Ontario, M5S 1A1, Canada

A spectroscopic and structural examination of the platinum(II) co-ordination chemistry of bis(diphenylphosphino)amine (dppa) and bis(diphenylphosphino)methylamine (dppma) has been made. The complexes  $[\text{Pt}(\text{dppa})\text{Cl}_2]$ ,  $[\text{Pt}(\text{dppma})\text{Cl}_2]$ ,  $[\text{Pt}(\text{dppa})(\text{CN})_2]$ ,  $[\text{Pt}(\text{dppma})(\text{CN})_2]$ ,  $[\text{Pt}(\text{dppa})_2]^{2+}$  and  $[\text{Pt}(\text{dppma})_2]^{2+}$  as the chloride, iodide and tetrafluoroborate salts,  $[\text{Pt}(\text{Ph}_2\text{PNPPh}_2)_2]$ , *trans*- $[\text{Pt}(\text{dppa}-P)_2(\text{CN})_2]$  and  $[\text{Pt}_2(\mu\text{-dppa})_2(\text{CN})_2]$  have been prepared. The solid-state structures of  $[\text{Pt}(\text{dppa})_2][\text{BF}_4]_2 \cdot \text{MeCN}$ ,  $[\text{Pt}(\text{dppma})_2][\text{BF}_4]_2$  and *trans*- $[\text{Pt}(\text{dppa}-P)_2(\text{CN})_2]$  have been determined by X-ray crystallography. The crystallographic examination permits a critical evaluation of the nature of the strain in the four-membered rings formed by ligand chelation to a transition-metal centre. Structural and theoretical data suggest that bis(diphenylphosphino)amine chelate complexes should be more strained than the corresponding bis(diphenylphosphino)methane (dppm) complexes. The preference of Pt<sup>II</sup> for binding to dppa rather than dppm implies the formation of a stronger Pt–P bond in complexes of the former ligand.

The mono- and bis-chelated platinum complexes of bis(diphenylphosphino)methane (dppm),  $\text{Ph}_2\text{PCH}_2\text{PPh}_2$ , are well known and are easily synthesised. Complexes  $[\text{Pt}(\text{dppm})_2][\text{X}_2]$  (X = Cl, Br or I) and  $[\text{Pt}(\text{dppm})\text{R}_2]$  (R = alkyl, aryl or halide) have been prepared from several starting materials including *trans*- $[\text{Pt}(\text{SMe}_2)_2\text{Cl}_2]$ ,<sup>1</sup>  $\text{K}_2[\text{PtCl}_4]$ ,<sup>2</sup> *trans*- $[\text{PtCl}_2(\text{NCBu}^t)_2]$ <sup>3</sup> and  $[\text{Pt}(\text{cod})\text{Cl}_2]$ <sup>4</sup> (cod = cycloocta-1,5-diene). Despite the number of monomeric Pt<sup>II</sup>(dppm) complexes that have been synthesised, they have eluded crystallographic examination. This structural information may have aided in assessing the strain energy associated with the formation of four-membered chelate ring systems. Evidence of the presence of ring strain in these complexes has been largely confined to NMR spectroscopic investigations which have shown the <sup>1</sup>J(P–Pt) coupling constants to be consistently lower than, and the <sup>31</sup>P chemical shifts to be upfield of, those of less-strained complexes of dppe or  $\text{PPh}_2\text{Me}$ .<sup>5–9</sup> Bis(diphenylphosphino)methane also is used as a bidentate ligand to stabilise bridged bi- and poly-metallic transition-metal complexes in low oxidation states.

We have been studying the bidentate compound bis(diphenylphosphino)amine (dppa),  $\text{Ph}_2\text{PN}(\text{H})\text{PPh}_2$ , and its derivatives. Our preliminary theoretical<sup>10</sup> and crystallographic studies<sup>11</sup> on chelated complexes of bis(phosphino)amine ligands suggested that they should possess more ring-strain energy than that of the corresponding dppm complexes. This conclusion is based upon the observation<sup>11</sup> that the small bite angle of the chelating ligands compresses the P–N–P bond angle to approximately 100°. The *ab initio* study<sup>10</sup> suggested that this bending at the N atom, which in dppa is formally sp<sup>2</sup> hybridised, from the P–N–P bond angle of the free amine to that of the chelate geometry requires more energy than bending the sp<sup>3</sup>-hybridised backbone C atom of free dppm to the same angle. Thus monomeric complexes of substituted bis(diphosphino)amine (dpa) ligands should be good starting materials for dpa-bridged polymeric complexes as there should be a substantial reduction in ring strain as the ligand in the chelated complexes opens to bridge two metal centres.

A recent review of the co-ordination chemistry of diphos-

phinoamines reports few platinum(II) complexes of dppa or its derivatives.<sup>12</sup> In the only extensive investigation of the dppa co-ordination chemistry of Pt<sup>II</sup>, Usón *et al.*<sup>9</sup> did not observe significant differences in chemical behaviour between dppa and dppm in the syntheses of complexes of the type  $[\text{M}(\text{L-L})_x(\text{C}_6\text{F}_5)_2]$  (M = Pd<sup>II</sup> or Pt<sup>II</sup>, L–L = dppa or dppm, x = 1 or 2).

Our investigation of the platinum(II) co-ordination chemistry of the ligands dppa and bis(diphenylphosphino)methylamine (dppma),  $\text{Ph}_2\text{PN}(\text{Me})\text{PPh}_2$ , is presented in this paper. Crystallographic studies of several of the complexes were performed. In addition, we recently have reported the structures of  $[\text{Pt}(\text{dppma})\text{Cl}_2]$  and  $[\text{Pt}(\text{dppma})(\text{CN})_2]$ .<sup>11</sup> The structural effects of co-ordination upon the bis(phosphino)amine ligands, with particular regard to structural evidence of ring strain, are discussed. Despite the structural and theoretical evidence that dppa and dppma chelated complexes of Pt<sup>II</sup> are highly strained, we find that the mono- and bis-chelated complexes are very stable.

## Results and Discussion

*Syntheses of the Complexes.*—The synthetic routes to the complexes are summarised in Scheme 1. Addition of 1 equivalent of the ligands dppa, **a**, or dppma, **b**, to a  $\text{CH}_2\text{Cl}_2$  solution of  $[\text{Pt}(\text{cod})\text{Cl}_2]$  resulted in the formation of the monochelate complexes  $[\text{Pt}(\text{dppa})\text{Cl}_2]$  **1a** or  $[\text{Pt}(\text{dppma})\text{Cl}_2]$  **1b**, in very good yields. The insolubility of the isolated complex **1a** in organic solvents dictated the use of solid-state magic angle spinning (MAS) NMR spectroscopy ‡ for the determination of its <sup>31</sup>P chemical shift and <sup>1</sup>J(P–Pt) coupling constant. This insolubility prevented the study of its subsequent reaction chemistry. The greater solubility of the iodo analogue of **1a** permitted its reaction with 2 equivalents of NaCN to yield the *cis*-cyano complex  $[\text{Pt}(\text{dppa})(\text{CN})_2]$  **2a**. The complex  $[\text{Pt}(\text{dppma})(\text{CN})_2]$  **2b** was synthesised in an analogous fashion using **1b** as the starting material. The <sup>31</sup>P NMR spectroscopic and mass spectrometric data of these mono(chelate) complexes are given in Table 1. As **2a** was not crystallographically characterised its composition was confirmed by elemental

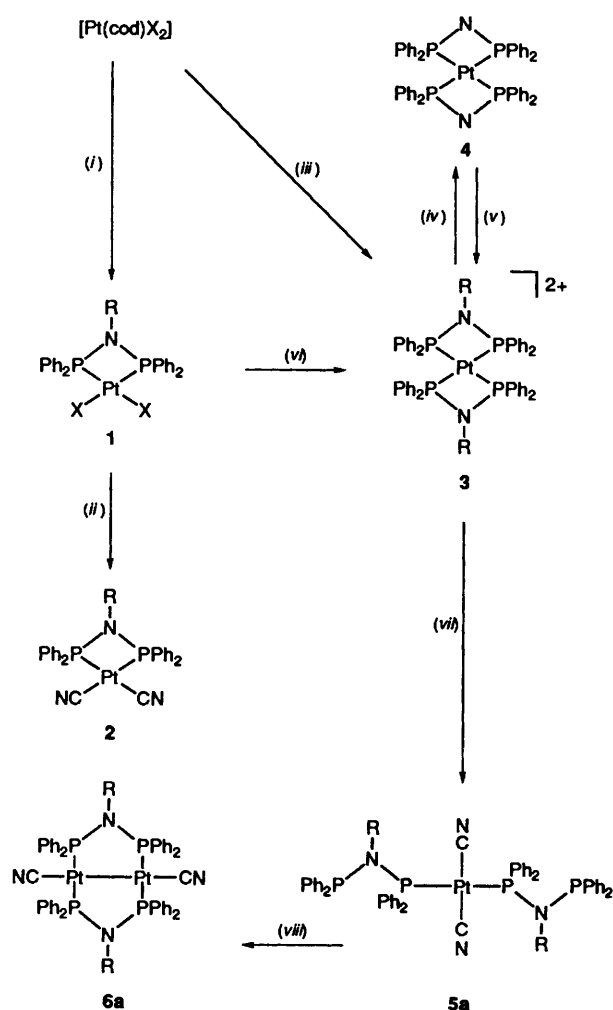
† Supplementary data available (No. SUP 57045, 3 pp.): variable-temperature <sup>31</sup>P-{<sup>1</sup>H} NMR spectra. See Instructions for Authors, *J. Chem. Soc., Dalton Trans.*, 1995, Issue 1, pp. xxv–xxx.

‡ The assistance of Professor P. M. MacDonald in the acquisition of the MAS NMR spectrum is gratefully acknowledged.

**Table 1** Solution  $^{31}\text{P}$  NMR spectroscopic<sup>a</sup> and FAB mass spectrometric<sup>b</sup> molecular ion data for complexes 1–6

Complex	$\delta^c$	$\Delta\delta^d$	$ ^1J(\text{P-Pt}) /\text{Hz}$	Molecular ion ( $m/z$ )	
<b>1a</b> <sup>e</sup>	-5.2	-46.8	3130		
<b>1b</b>	15.6	-55.8	3300	$[\text{1b} - \text{Cl}]^+$	(630)
<b>2a</b> <sup>f</sup>	3.5	-38.1	2174	$[\text{2a}]^+$	(633)
<b>2b</b>	26.1	-45.3	2249	$[\text{2b}]^+$	(647)
<b>3a</b> <sup>g</sup>	22.0	-19.3	2100	$[\text{3a} - \text{H}_2]^+$	(964)
<b>3b</b> <sup>g</sup>	39.6	-31.8	2130	$[\text{3b}]^+$	(994)
<b>4</b>	-17.4	-59.0	1660	$[\text{4}]^+$	(964)
<b>5a</b> <sup>h</sup>	43.6 ( $\text{P}_{\text{Pt}}$ ) 27.3 ( $\text{P}_{\text{free}}$ )	2.0	2436 <sup>i</sup>	$[\text{5a} - \text{HCN}]^+$	(991)
<b>6a</b>	53.9	—	2969 <sup>j</sup>	$[\text{6a}]^+$	(1213)

<sup>a</sup> In  $\text{CH}_2\text{Cl}_2$  solvent at 20 °C. <sup>b</sup> Xenon gas as ionising source at 8 kV and 1 mA; 3-nitrobenzyl alcohol matrix. <sup>c</sup> Values relative to 85%  $\text{H}_3\text{PO}_4$ . <sup>d</sup> Defined as  $\delta_{\text{complex}} - \delta_{\text{ligand}}$ . <sup>e</sup>  $\delta_{\text{dppa}}$  41.6,  $\delta_{\text{dppma}}$  71.4. <sup>f</sup> Solid state. <sup>g</sup> In  $\text{Me}_2\text{SO}$  solvent. <sup>h</sup> As the  $[\text{BF}_4]^-$  salt. <sup>i</sup> Obtained at -90 °C. <sup>j</sup>  $|^2J(\text{P}_{\text{Pt}}-\text{P}_{\text{free}})| + ^4J(\text{P}_{\text{Pt}}-\text{P}_{\text{free}}) = 22$  Hz,  $^3J(\text{P}_{\text{free}}-\text{Pt})$  not resolved. <sup>k</sup>  $|^2J(\text{P-Pt})| = 89$ ,  $|^2J(\text{P-P}')| = |^2J(\text{P-P''})| = 714$ ,  $|^2J(\text{P-P''})| = |^2J(\text{P'-P''})| = 56$ ,  $|^3J(\text{P-P''})| = |^3J(\text{P'-P''})| = 34$ ,  $|^1J(\text{Pt-Pt})| \approx 8500$  Hz.



**Scheme 1** Synthetic routes to products 1–6. (i)  $\text{Ph}_2\text{PNRPPH}_2$  ( $\text{R} = \text{H}$  a or Me b),  $\text{X} = \text{Cl}$  or I; (ii)  $2\text{CN}^-$ ,  $\text{R} = \text{Me}$  ( $\text{X} = \text{Cl}$  or I) or  $\text{H}$  ( $\text{X} = \text{I}$ ); (iii)  $2 \text{Ph}_2\text{PNRPPH}_2$ ,  $\text{X} = \text{Cl}$  or I; (iv)  $\text{R} = \text{H}$ ,  $\text{LiNEt}_2$ ; (v)  $\text{HBF}_4$  ( $\text{R} = \text{H}$ ) or  $\text{MeI}$  ( $\text{R} = \text{Me}$ ); (vi)  $\text{Ph}_2\text{PN}(\text{Me})\text{PPH}_2$ ; (vii)  $2\text{CN}^-$ ,  $\text{R} = \text{H}$ ; (viii)  $[\text{Pt}(\text{cod})_2]$

analysis. The crystal structures of complexes **1b** and **2b** have been reported.<sup>11</sup>

A greater stability of the bis(phosphino)amine chelates of  $\text{Pt}^{\text{II}}$ , with respect to the dppm analogues, is evident in their respective mass spectra. The molecular-ion peak, which is present in the FAB mass spectra of complexes **1b** and **2** (Table 1), is absent

in those of  $[\text{Pt}(\text{dppm})\text{Cl}_2]$  and  $[\text{Pt}(\text{dppm})(\text{CN})_2]$  as these complexes dimerise under FAB conditions.<sup>13</sup> This stability is in contrast to our work which showed<sup>11</sup> the ligands to be highly strained when chelating to  $\text{Pt}^{\text{II}}$  and suggested that bending of dppa to the chelating geometry should destabilise it to a greater degree than a similar bending of dppm.<sup>10</sup>

**Synthesis and Solid-state Structure of the Bis(chelate) Complexes  $[\text{Pt}(\text{dppa})_2][\text{BF}_4]_2 \cdot \text{MeCN}$ , and  $[\text{Pt}(\text{dppma})_2][\text{BF}_4]_2$ .**—The bis(chelate) complexes of  $\text{Pt}^{\text{II}}$ , **3**, are obtained as the chloride salts from the addition of  $[\text{Pt}(\text{cod})\text{Cl}_2]$  to a solution of 2 equivalents of the amines. The chloride salt of  $[\text{Pt}(\text{dppma})_2]^{2+}$  **3b** also can be generated from the reaction of **1b** with a second equivalent of dppma. Complexes **3** were metathesised to obtain the  $[\text{BF}_4]^-$  salts as the halide salts of **3b** were found to undergo a further reaction with trace quantities of water.<sup>14</sup> The  $[\text{BF}_4]^-$  counter ions also provided crystalline samples of the bis(chelate) complexes suitable for crystallographic investigation.

The crystal structures consist of discrete ions of  $[\text{Pt}(\text{dppa})_2]^{2+}$  **3a** or  $[\text{Pt}(\text{dppma})_2]^{2+}$  **3b**, with their respective  $[\text{BF}_4]^-$  counter ions. Crystal data are presented in Table 2 and positional parameters in Tables 3 and 4. Although the crystals of **3a** and **3b** are not isomorphic, both dications possess a crystallographically imposed centre of symmetry. The crystals of **3a** contained 1 equivalent of acetonitrile as solvent of crystallisation. The ORTEP<sup>15</sup> diagrams of the cations **3a** and **3b** are shown in Figs. 1 and 2, selected bond distances and angles in Tables 5 and 6, respectively. The  $^{31}\text{P}$  NMR spectroscopic and mass spectrometric data of the complexes **3** are in Table 1.

A separation of 2.848(9) Å between the N atom of the dppa ligand in **3a** and the F(3) atom of the  $[\text{BF}_4]^-$  counter ion suggests the presence of a hydrogen-bonding interaction. Hydrogen bonding involving co-ordinated dppa has been observed in the solid-state structure of  $[\text{Rh}_2(\mu\text{-CO})(\mu\text{-Cl})(\mu\text{-dppa})_2(\text{CO})_2]\text{Cl} \cdot \text{MeOH}$ <sup>16</sup> and has been offered as an explanation of the broadened  $\nu(\text{N-H})$  absorptions in the solid-state IR spectrum of  $[(\text{C}_6\text{F}_5)_2\text{Pd}(\mu\text{-dppa})_2\text{Ag}][\text{ClO}_4]$ .<sup>9a</sup> The analogous interaction between the counter ion of **3b** and the ligand's methyl hydrogen atoms does not occur.

The Pt–P bond lengths of complex **3b** are equivalent with an average length of 2.298(1) Å. No chemical significance is attached to the significantly distinct ( $3.3\sigma$ ) distances of 2.293(2) and 2.303(2) Å found for the Pt–P bonds in **3a**, as these values do not differ from the average distance in **3b**. The  $^{31}\text{P}$  NMR spectra of **3** show the phosphorus nuclei within each complex to be equivalent in solution. The average Pt–P distance [2.298(4) Å] for complexes **3** being significantly longer than the Pt–P bond lengths of the monochelate platinum complexes<sup>11</sup> **1b** [2.206(4) Å] and **2b** [2.268(2) Å] is consistent with the greater *trans* influence<sup>17</sup> of the phosphine ligands than that of

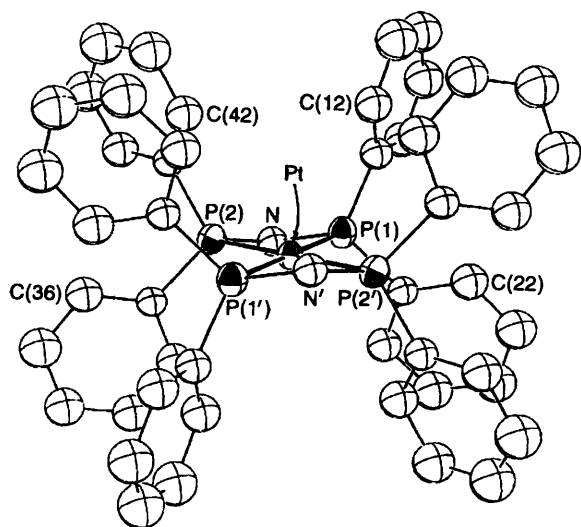


Fig. 1 An ORTEP diagram of  $[\text{Pt}(\text{dppa})_2]^{2+}$  **3a** as its  $\text{BF}_4^-$  salt, showing the atom numbering scheme. Thermal ellipsoids represent 50% probability contours. Hydrogen atoms have been removed for clarity

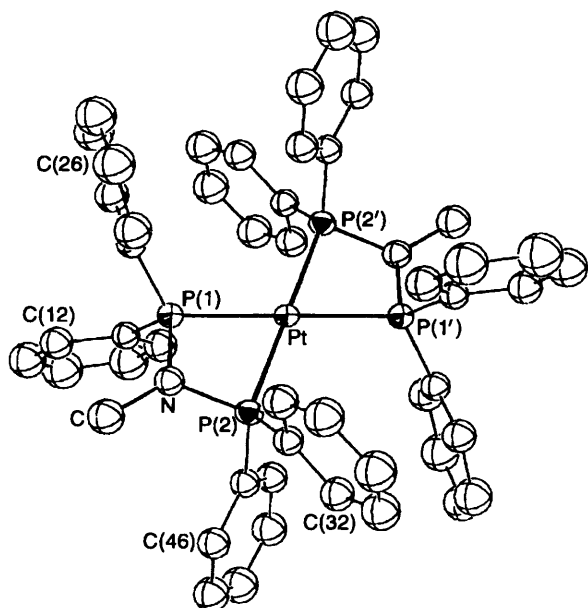


Fig. 2 An ORTEP diagram of  $[\text{Pt}(\text{dppma})_2]^{2+}$  **3b** as its  $\text{BF}_4^-$  salt, showing the atom numbering scheme. Thermal ellipsoids represent 50% probability contours. Hydrogen atoms have been removed for clarity

the chloride (**1b**) and cyanide (**2b**) ligands. The P–N bond distances of both complexes, like those of the mono(chelate) complexes, are statistically equivalent and indistinguishable from the values observed in free dppa.<sup>18</sup> The bond lengths and angles of the acetonitrile solvate of **3a**, and the phenyl groups and counter ions of both complexes, are normal.<sup>19</sup>

While planarity of the four P atoms and the platinum centre of complexes **3** is crystallographically imposed, the square-planar geometry is significantly distorted in the formation of the four-membered rings with P–Pt–P bond angles of 69.90(7) and 69.76(5)° in **3a** and **3b**, respectively. The P–N–P bond angles of the complexes [102.7(4) **3a** and 101.6(2)° **3b**; cf. 118.9(2)° in dppa<sup>18</sup>] also reflect the ring strain present. In contrast to the highly unfavourable<sup>20</sup> distortions toward tetrahedral geometry observed<sup>21</sup> in the complex  $[\text{Pt}\{\text{P}(\text{OMe})_3\}_4]^{2+}$  of one of the smallest P-donor ligands,<sup>22</sup> the ideally planar geometry about the metal centre of **3** suggests that the incorporation of the co-ordinated phosphine groups into two strained four-membered rings confers a reduction in interligand non-bonded interactions

in these complexes. The decrease in intramolecular steric contact is believed to permit the dpa ligand to optimise its interaction with the metal centre, within the limits imposed by the constraints of the ligand backbone. The significantly shorter Pt–P bond length of **3a** in comparison to that of the monodentate complex  $\text{trans-}[\text{Pt}(\text{dppa-}P)_2(\text{CN})_2]$  **5a** (see below) in which ring strain is absent supports this hypothesis and further suggests that the chelated phosphorus atoms achieve effective radial orbital overlap with the platinum(II) centre despite their unusual position relative to it.

*Crystallographic Evidence of Ring Strain in the Chelate Complexes.*—The displacements of the methyl carbon atoms from the P–N–P plane of the ligands in the crystal structures of the chelated complexes of dppma (Table 7) indicate that planarity at the nitrogen centre, as observed in the solid-state structure of  $\text{NPr}'(\text{PPh}_2)_2$ ,<sup>23</sup> is not maintained upon chelation. The degree of pyramidal character of the nitrogen centre is more clearly demonstrated when expressed as a percentage as calculated in Table 7. While the nitrogen atoms remain best described in the valence-bond model as  $\text{sp}^2$  hybridised, their explicit deformation towards a pyramidal configuration is the result of the ring strain present in these complexes. Preliminary *ab initio* calculations, in simulating the structural effects of co-ordination of the ligand to the platinum(II) cation, have shown that protonation of both phosphorus atoms of  $\text{PH}_2\text{N}(\text{H})\text{PH}_2$  and bending of the ligand to the chelating geometry ( $C_{2v}$  symmetry, P–N–P angle 90°) are necessary and sufficient to achieve a modestly pyramidal configuration at the nitrogen centre.<sup>14</sup> Ring strain is thereby reduced in the chelated complexes as the nitrogen centres incorporate greater p-orbital character into their bonding with the phosphorus atoms.

The N atom's pyramidal character also is evident structurally in the deviation from coplanarity of the  $\text{P}_2\text{N}$  plane of the ligands from the plane defined by the Pt atom and the co-ordinated phosphorus atoms (Table 7). Non-bonding interactions within the ligand are minimised by this displacement of the non-planar nitrogen atom which allows the methyl substituents to maintain a staggered configuration with respect to the phenyl substituents of the phosphino groups.<sup>24</sup> The reduction in dihedral angle which accompanies the replacement of the methyl group of complex **3b** with the proton of **3a** supports this hypothesis.

The indistinguishable Pt–P bond lengths observed between the complexes **3**, in the solid state, is reflected in the similar magnitude of their  $^1J(\text{P-Pt})$  coupling constants in solution (Table 1). Comparison of the **1b**  $^1J(\text{P-Pt})$  coupling constant of 3300 Hz with the value of 3617 Hz observed for  $[\text{Pt}(\text{dppe})\text{Cl}_2]^4$  (dppe =  $\text{Ph}_2\text{PCH}_2\text{CH}_2\text{PPh}_2$ ) suggests that the reduction in coupling that has been attributed to ring strain<sup>6</sup> in the complexes of dppm also is present in the diphosphinoamine complexes.

The  $^1J(\text{P-Pt})$  coupling constants of the complexes **1** and **3** are substantially larger than those of 3076 and 1962 Hz observed for the corresponding dppm complexes  $[\text{Pt}(\text{dppm})\text{Cl}_2]^4$  and  $[\text{Pt}(\text{dppm})_2(\text{BPh}_4)_2]$ ,<sup>25</sup> respectively. As s-orbital character is the most important variable in determining the magnitude of the coupling between a metal nucleus and a directly bonded phosphorus atom,<sup>26</sup> the data are consistent with a greater contribution of s-orbital character to the Pt–P interaction from the phosphorus lone pair of dppa than from that of dppm.

A further manifestation of this disparity in s-character in the platinum–phosphorus interaction is apparent in the relative Pt–P bond strengths between complex **3a** and  $[\text{Pt}(\text{dppm})_2]^{2+}$ . We observe a selectivity of dppa over dppm in chelation to platinum(II) centres. Addition of 2 equivalents of dppa to the chloride salt of  $[\text{Pt}(\text{dppm})_2]^{2+}$ , at 23 °C, results in exclusive formation of **3a**, as observed by  $^{31}\text{P}$  NMR spectroscopy.

Within the three pairs of complexes **1–3**, a greater amount of s character is evident in the P–Pt interaction of the dppma derivatives which exhibit  $^1J(\text{P-Pt})$  coupling constants which

**Table 2** X-Ray experimental details for the complexes [Pt(dppa)<sub>2</sub>][BF<sub>4</sub>]<sub>2</sub>·MeCN, [Pt(dppma)<sub>2</sub>][BF<sub>4</sub>]<sub>2</sub> and **5a**

	[Pt(dppa) <sub>2</sub> ][BF <sub>4</sub> ] <sub>2</sub> ·MeCN	[Pt(dppma) <sub>2</sub> ][BF <sub>4</sub> ] <sub>2</sub>	<b>5a</b>
Empirical formula	C <sub>52</sub> H <sub>48</sub> B <sub>2</sub> F <sub>8</sub> N <sub>4</sub> P <sub>4</sub> Pt	C <sub>50</sub> H <sub>46</sub> B <sub>2</sub> F <sub>8</sub> N <sub>2</sub> P <sub>4</sub> Pt	C <sub>50</sub> H <sub>42</sub> N <sub>4</sub> P <sub>4</sub> Pt
<i>M</i>	1221.58	1167.53	1017.91
Space group (crystal system)	<i>P</i> $\bar{1}$ (triclinic)	<i>P</i> 2 <sub>1</sub> / <i>n</i> (monoclinic)	<i>P</i> 2 <sub>1</sub> / <i>c</i> (monoclinic)
<i>a</i> /Å	10.060(6)	11.114(4)	8.637(2)
<i>b</i> /Å	11.189(3)	15.901(4)	17.188(2)
<i>c</i> /Å	12.972(3)	14.544(2)	15.456(2)
$\alpha$ /°	112.42(2)	90	90
$\beta$ /°	102.55(4)	100.62(2)	94.45(1)
$\gamma$ /°	93.25(3)	90	90
<i>U</i> /Å <sup>3</sup>	1302(2)	2526(2)	2288(1)
<i>Z</i>	1	2	2
Crystal dimensions/mm	0.18 × 0.10 × 0.18	0.28 × 0.06 × 0.28	0.10 × 0.25 × 0.08
<i>D</i> <sub>c</sub> /g cm <sup>-3</sup>	1.56	1.54	1.48
<i>F</i> (000)	608	1160	1016
$\mu$ /cm <sup>-1</sup>	29.1	30.0	32.7
2 $\theta$ range/°	2–44	2–44	2–50
Unique reflections:			
measured	2649	6377	4298
<i>I</i> ≥ 3 $\sigma$ ( <i>I</i> )	2321	3651	2639
Number of parameters	177	169	133
<i>R</i>	0.042	0.036	0.030
<i>R</i> '	0.058	0.045	0.040
E.s.d. of observation of unit weight	1.65	1.20	1.12
Highest peak in final Fourier-difference map/e Å <sup>-3</sup>	1.81	1.06	0.83

**Table 3** Positional parameters of [Pt(dppa)<sub>2</sub>][BF<sub>4</sub>]<sub>2</sub>·MeCN

Atom	<i>x</i>	<i>y</i>	<i>z</i>
Pt	0	0	0
P(1)	0.1466(3)	-0.1128(2)	0.0756(2)
P(2)	0.2041(3)	0.1352(2)	0.1134(2)
N	0.2807(8)	0.0073(7)	0.1225(6)
C(11)	0.118(1)	-0.1463(9)	0.1938(7)
C(12)	0.007(1)	-0.1046(9)	0.2367(8)
C(13)	-0.011(1)	-0.123(1)	0.336(1)
C(14)	0.082(1)	-0.182(1)	0.384(1)
C(15)	0.190(1)	-0.224(1)	0.3441(9)
C(16)	0.209(1)	-0.207(1)	0.2478(8)
C(21)	0.180(1)	-0.2619(8)	-0.0286(7)
C(22)	0.089(1)	-0.374(1)	-0.0575(8)
C(23)	0.095(1)	-0.487(1)	-0.1496(9)
C(24)	0.193(1)	-0.489(1)	-0.2080(9)
C(25)	0.282(1)	-0.380(1)	-0.1793(9)
C(26)	0.277(1)	-0.2621(9)	-0.0882(8)
C(31)	0.295(1)	0.2184(8)	0.0504(7)
C(32)	0.343(1)	0.145(1)	-0.0425(8)
C(33)	0.392(1)	0.203(1)	-0.1065(9)
C(34)	0.389(1)	0.334(1)	-0.0797(9)
C(35)	0.342(1)	0.406(1)	0.0114(9)
C(36)	0.293(1)	0.3495(9)	0.0773(8)
C(41)	0.197(1)	0.2511(8)	0.2521(7)
C(42)	0.075(1)	0.2486(9)	0.2837(8)
C(43)	0.064(1)	0.338(1)	0.3903(9)
C(44)	0.177(1)	0.429(1)	0.461(1)
C(45)	0.299(1)	0.434(1)	0.431(1)
C(46)	0.312(1)	0.3436(9)	0.3274(8)
F(1)	0.343(1)	0.7385(8)	0.5937(7)
F(2)	0.420(1)	0.9513(8)	0.6526(7)
F(3)	0.4405(8)	0.8667(8)	0.7779(6)
F(4)	0.2359(9)	0.890(1)	0.6954(9)
B	0.357(2)	0.858(1)	0.677(1)
N(1)	0.479(2)	0.343(1)	0.676(1)
C(1)	0.422(2)	0.255(1)	0.604(1)
C(2)	0.349(2)	0.140(2)	0.505(1)

**Table 4** Positional parameters of [Pt(dppma)<sub>2</sub>][BF<sub>4</sub>]<sub>2</sub>

Atom	<i>x</i>	<i>y</i>	<i>z</i>
Pt	0	0	0
P(1)	-0.078 9(1)	0.118 86(9)	0.056 6(1)
P(2)	-0.208 1(1)	0.005 9(1)	-0.050 97(9)
N	-0.224 5(4)	0.081 5(3)	0.027 4(3)
C	-0.338 2(6)	0.127 4(4)	0.036 7(5)
C(11)	-0.063 4(5)	0.216 7(4)	-0.002 1(4)
C(12)	-0.119 2(6)	0.289 9(4)	0.021 1(5)
C(13)	-0.108 5(6)	0.362 9(5)	-0.028 3(5)
C(14)	-0.046 1(7)	0.364 6(5)	-0.098 8(6)
C(15)	0.013 4(7)	0.293 2(5)	-0.122 2(6)
C(16)	0.003 0(6)	0.218 5(4)	-0.074 4(5)
C(21)	-0.038 1(5)	0.137 2(4)	0.180 3(4)
C(22)	-0.089 9(6)	0.088 7(5)	0.241 7(5)
C(23)	-0.036 8(7)	0.092 3(5)	0.336 8(5)
C(24)	0.062 8(7)	0.141 0(5)	0.367 9(5)
C(25)	0.111 7(7)	0.189 6(5)	0.307 2(5)
C(26)	0.061 1(6)	0.188 0(4)	0.211 1(5)
C(31)	-0.298 2(5)	-0.084 5(4)	-0.034 3(4)
C(32)	-0.340 2(6)	-0.136 2(4)	-0.110 2(4)
C(33)	-0.391 0(6)	-0.214 7(5)	-0.096 5(5)
C(34)	-0.394 5(7)	-0.240 8(5)	-0.007 5(6)
C(35)	-0.355 2(6)	-0.189 3(5)	0.068 2(5)
C(36)	-0.305 5(6)	-0.111 2(4)	0.056 5(5)
C(41)	-0.261 1(5)	0.041 3(4)	-0.168 9(4)
C(42)	-0.385 5(5)	0.057 8(4)	-0.201 8(4)
C(43)	-0.423 0(6)	0.086 2(5)	-0.293 4(5)
C(44)	-0.338 5(7)	0.096 5(5)	-0.350 2(5)
C(45)	-0.216 6(6)	0.079 6(5)	-0.319 2(5)
C(46)	-0.178 2(5)	0.052 6(4)	-0.227 2(4)
F(1)	0.268 5(4)	0.083 7(4)	-0.289 8(4)
F(2)	0.091 5(4)	0.119 8(4)	-0.252 5(3)
F(3)	0.207 0(6)	0.216 5(4)	-0.305 0(5)
F(4)	0.112 7(7)	0.118 7(5)	-0.401 4(4)
B	0.169 3(8)	0.134 0(6)	-0.312 7(7)

are 170, 75 and 30 Hz respectively larger than those of their dppa analogues. This effect diminishes with the increasing influence of the *trans* ligand.<sup>17</sup>

The effect of ring strain also is evident in the chemical shift of the chelated complexes of dppa and dppma when expressed relative to the chemical shift of the respective free amines to

obtain the parameter  $\Delta\delta^7$  (Table 1). As observed in the platinum(II) complexes of dppm,<sup>5–8</sup> the effect of ring strain is then evident as large negative values of  $\Delta\delta$  (–19 to –59)<sup>6,8</sup> in comparison to that of 2.0 for *trans*-[Pt(dppa-*P*)<sub>2</sub>(CN)<sub>2</sub>] **5a** in which ring strain is absent. An increase in the respective difference in  $\Delta\delta$  values between the derivative pairs of **1–3** accompanies the decrease in the <sup>1</sup>*J*(P–Pt) coupling constant.

The bond angles about the phosphorus atoms of the chelated

**Table 5** Selected bond distances (Å) and angles (°) for [Pt-(dppa)<sub>2</sub>][BF<sub>4</sub>]<sub>2</sub>·MeCN

Pt-P(1)	2.293(2)	P(1)-C(21)	1.806(8)
Pt-P(2)	2.303(2)	P(2)-N	1.694(6)
P(1)-N	1.677(7)	P(2)-C(31)	1.786(8)
P(1)-C(11)	1.788(8)	P(2)-C(41)	1.793(8)
P(1)-Pt-P(2)	69.90(7)	Pt-P(2)-N	91.9(2)
Pt-P(1)-N	92.7(2)	Pt-P(2)-C(31)	117.9(3)
Pt-P(1)-C(11)	119.3(3)	Pt-P(2)-C(41)	115.3(3)
Pt-P(1)-C(21)	115.4(3)	N-P(2)-C(31)	110.5(3)
N-P(1)-C(11)	110.0(3)	N-P(2)-C(41)	112.1(3)
N-P(1)-C(21)	110.8(3)	C(31)-P(2)-C(41)	108.3(4)
C(11)-P(1)-C(21)	107.7(4)	P(1)-N-P(2)	102.7(4)

**Table 6** Selected bond distances (Å) and angles (°) for [Pt-(dppma)<sub>2</sub>][BF<sub>4</sub>]<sub>2</sub>

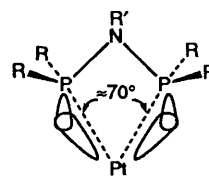
Pt-P(1)	2.299(1)	P(2)-N	1.690(5)
Pt-P(2)	2.297(1)	P(2)-C(31)	1.793(5)
P(1)-N	1.702(4)	P(2)-C(41)	1.798(5)
P(1)-C(11)	1.798(5)	N-C	1.486(7)
P(1)-C(21)	1.796(6)		
P(1)-Pt-P(2)	69.76(5)	Pt-P(2)-C(31)	118.5(2)
Pt-P(1)-N	91.8(2)	Pt-P(2)-C(41)	117.0(2)
Pt-P(1)-C(11)	117.7(2)	N-P(2)-C(31)	110.3(2)
Pt-P(1)-C(21)	116.7(2)	N-P(2)-C(41)	111.3(3)
N-P(1)-C(11)	110.7(2)	C(31)-P(2)-C(41)	106.7(3)
N-P(1)-C(21)	111.1(2)	P(1)-N-P(2)	101.6(2)
C(11)-P(1)-C(21)	107.9(3)	P(1)-N-C	126.2(4)
Pt-P(2)-N	92.2(2)	P(2)-N-C	127.6(4)

**Table 7** Displacements of the methyl carbon atom from the P<sub>2</sub>N plane of the ligand, percentage pyramidal character of the nitrogen atom and dihedral angles between the PtP<sub>2</sub> and P<sub>2</sub>N planes in complexes [Pd(dppma)Cl<sub>2</sub>], **1b**, **2b**, **3a** and **3b**

Compound	Displacement/Å	Pyramidal character <sup>a</sup> (%)	Dihedral angle/°
NPr'(PPh <sub>2</sub> ) <sub>2</sub> <sup>b</sup>	n.a.	0.6(20)	—
[Pd(dppma)Cl <sub>2</sub> ] <sup>c</sup>	0.398(7)	11.4(15)	6.5
<b>1b</b>	0.343(25)	9.2(51)	5.1
<b>2b</b>	0.396(12)	10.2(24)	5.8
<b>3a</b>	— <sup>d</sup>	— <sup>d</sup>	17.8
<b>3b</b>	0.465(9)	14.6(19)	22.7

n.a. = Not applicable. <sup>a</sup> Defined as follows: let ( $\Sigma\theta$ ) be the sum of the three angles,  $\theta$ , between amine substituents of the ligand. For an ideally planar nitrogen centre ( $\Sigma\theta$ )<sub>plan</sub> = 360° while for an ideally tetrahedral nitrogen centre ( $\Sigma\theta$ )<sub>tet</sub> = 328.5°. The percentage pyramidal character in a given complex may then be expressed as:  $[(\Sigma\theta)_{plan} - (\Sigma\theta)_{complex}] / [(\Sigma\theta)_{plan} - (\Sigma\theta)_{tet}] \times 100\% = [360^\circ - (\Sigma\theta)_{complex}] / [31.5^\circ] \times 100\%$ .  
<sup>b</sup> Ref. 23. <sup>c</sup> Ref. 11. <sup>d</sup> Methyl group not present in dppa ligand.

complexes reflect a distinct difference in the nature of their interaction with the platinum centre from that with its remaining three substituents. The average C-P-X (X = C or N) bond angle of 108.6° ( $\sigma = 2.3^\circ$ ) between the native substituents of the chelated ligands of **1b**, **2b** and **3** is very similar to that of 106.7° ( $\sigma = 2.6^\circ$ ) observed about the co-ordinated phosphorus centre of the complex *trans*-[Pt(dppa-P)<sub>2</sub>(CN)<sub>2</sub>] **5a**. This suggests that the co-ordinated phosphorus atom does not undergo a dramatic change in hybridisation to accommodate the unusual bond angle to the metal centre in formation of the four-membered ring. Rather, the Pt-P bond in the chelate complexes may be better considered as an interaction of an approximately sp<sup>3</sup> hybridised orbital of the phosphorus atoms' lone pair of electrons with a platinum(n) orbital of formally dsp<sup>2</sup> character which also lies outside of the Pt-P vector as shown schematically in Fig. 3. The non-linear nature of the Pt-P interaction<sup>27</sup> offers a rationale, other than the presence of

**Fig. 3** Schematic representation of a non-linear interaction between platinum and phosphorus centres of the four-membered ring. The Pt-P internuclear vectors are denoted by dashed lines

more phosphorus p-orbital character in the Pt-P bond,<sup>6</sup> for the reduced <sup>1</sup>J(P-Pt) coupling observed for these complexes.

**Synthesis and Characterisation of the Deprotonated Complex [Pt{(Ph<sub>2</sub>P)<sub>2</sub>N}<sub>2</sub>] 4.**—Slow addition of a dimethylformamide (dmf) solution of lithium diethylamide to a dmf solution of complex **3a** results in the precipitation of [Pt{(Ph<sub>2</sub>P)<sub>2</sub>N}<sub>2</sub>] **4** as an air-stable white compound in good yield. The removal of the aminic protons was confirmed by the absence of the broad absorption band corresponding to the N-H stretches [ $\nu(\text{N-H}) \approx 3450\text{--}3650\text{ cm}^{-1}$  in Me<sub>2</sub>CO] of **3a** in the IR spectrum of **4**. The compounds are differentiable notably in their FAB mass spectra by the presence of those peaks corresponding to the double charged cation which are present for **3a** but which are absent in the deprotonated compound. The composition of **4** was confirmed by elemental analysis, in the absence of crystallographic characterisation. The <sup>31</sup>P NMR spectrum (Table 1) is not in agreement with that previously reported<sup>28</sup> for an air-stable yellow solid isolated from the reaction of lithium bis(diphenylphosphino)amide with [K<sub>2</sub>PtCl<sub>4</sub>]-PMe<sub>3</sub>.

Reprotonation of complex **4** was effected, without decomposition,<sup>28</sup> by the addition of HBF<sub>4</sub> as a diethyl ether solution. Compound **3b** could be recovered as the iodo salt in quantitative yield from the reaction of **4** with the mild methylating agent MeI in CH<sub>2</sub>Cl<sub>2</sub> or in neat MeI. Several attempts at obtaining reaction at the deprotonated nitrogen centre with such diverse species as [Pt(cod)Cl<sub>2</sub>], MoCl<sub>6</sub>, [W(CO)<sub>5</sub>(thf)] (thf = tetrahydrofuran) and CS<sub>2</sub> proved unsuccessful.

**Synthesis, Solution Behaviour and Solid-state Structure of *trans*-[Pt(dppa-P)<sub>2</sub>(CN)<sub>2</sub>] 5a.**—Cleavage of the Pt-P bond of the chelated ligand to obtain a  $\sigma$  mode of co-ordination was achieved in the synthesis of *trans*-[Pt(dppa-P)<sub>2</sub>(CN)<sub>2</sub>] **5a** by reaction of complex **3a** with 2 equivalents of NaCN.<sup>3</sup> Spectroscopic characterisation of **5a** required a variable-temperature <sup>31</sup>P-{<sup>1</sup>H} NMR study as the complex exhibits fluxional behaviour at room temperature. The process is consistent with an intramolecular exchange of the ligand's unco-ordinated phosphine with that which is co-ordinated to the platinum centre. The analogous dppm complex *trans*-[Pt(dppm-P)<sub>2</sub>(CN)<sub>2</sub>] demonstrates parallel behaviour,<sup>3</sup> while *trans*-[Pt(dppa-P)<sub>2</sub>(C<sub>6</sub>F<sub>5</sub>)<sub>2</sub>] is apparently static in this respect.<sup>9</sup>

The variable-temperature NMR spectra obtained over a range of 130 °C have been deposited as SUP 57045. The fluxional process which complex **5a** undergoes at ambient temperatures is effectively arrested at -90 °C thereby permitting the unambiguous characterisation of the product. The magnitude of the <sup>1</sup>J(P-Pt) coupling constant of the co-ordinated phosphorus atom (Table 1) and the single IR absorption attributed to the stretch of the cyano group [ $\nu(\text{C}\equiv\text{N}) 2126\text{ cm}^{-1}$  in CH<sub>2</sub>Cl<sub>2</sub> (20 °C)] are consistent with the dppa ligands of **5a** possessing a *trans* arrangement about the platinum centre.<sup>3</sup> The virtually coupled triplet of the central resonance of the co-ordinated phosphorus atom which arises from the strong <sup>2</sup>J(P-P) coupling between the co-ordinated phosphorus atoms supports the stereochemical assignment and has been observed for *trans*-[Pt(dppm-P)<sub>2</sub>(CN)<sub>2</sub>]<sup>3</sup> and *trans*-[Pt(dppa-P)<sub>2</sub>(C<sub>6</sub>F<sub>5</sub>)<sub>2</sub>].<sup>9</sup> The chemical shift associated with the unco-ordinated phosphorus atom ( $\delta 27.3$ ) is similar to that of  $\delta 29.2$  observed for *trans*-[Pt(dppa)<sub>2</sub>(C<sub>6</sub>F<sub>5</sub>)<sub>2</sub>].<sup>9</sup>

As the solution is allowed to warm to  $-80\text{ }^{\circ}\text{C}$  the fine P-P coupling disappears as the resonances begin to broaden due to the onset of the fluxional process. The increased rate of exchange brought about by further heating of the solution gives rise to continued broadening and converging of the peaks until the resonances of the free and co-ordinated moieties of the ligands coalesce at  $\delta \approx 35$  at  $0\text{ }^{\circ}\text{C}$ . The fast-exchange limit was not attainable due to the conversion of complex **5a** into uncharacterised products at temperatures higher than  $40\text{ }^{\circ}\text{C}$ .

The addition of a small quantity of dppa at  $40\text{ }^{\circ}\text{C}$  results in the loss of the exchange-averaged  $^{195}\text{Pt}$  coupling and migration of the averaged chemical shift of complex **5a** toward that of free dppa ( $\delta$  41.6) as intermolecular exchange of dppa competes with the fluxional process.

The inability to isolate *trans*-[Pt(dppma-P)<sub>2</sub>(CN)<sub>2</sub>] **5b** as the product of the reaction of complex **3b** with methanolic NaCN reveals a significant difference in the co-ordinative properties of dppa and dppma. The latter proves to be a superior chelator of Pt<sup>II</sup> as the monochelate complex **2b** and free dppma represent the major initial products of the reaction, as observed by  $^{31}\text{P}$  NMR spectroscopy. The remaining species is thought to be the cyanide salt of the bis(chelate) starting material; its  $|^1J(\text{P-Pt})|$  coupling constant of 1793 Hz is too large to represent the fast-exchange limit of an intramolecular phosphine exchange process of the type observed in **5a** [*cf.* exchange-averaged  $^1J(\text{P-Pt}) \approx 1240$  Hz]. The cyanide salt of [Pt(dppm)<sub>2</sub>]<sup>2+</sup> is observed<sup>3</sup> in nitromethane or nitrobenzene solutions of *trans*-[Pt(dppm-P)<sub>2</sub>(CN)<sub>2</sub>]. An intimate association of cyanide anion with **3b** in this salt is thought to be responsible for the faint yellow colour of the solution (solutions of **2b** and the [BF<sub>4</sub>]<sup>-</sup> salt of **3b** are both colourless) and the difference in chemical shift and coupling constant in comparison to the values of the [BF<sub>4</sub>]<sup>-</sup> salt of the starting material (Table 1). Counter ion association to obtain deeply coloured solutions has been shown to occur for the halide salts of **3b**.<sup>14</sup>

The *trans* configuration of the ligands in complex **5a** was confirmed crystallographically. Crystal data are given in Table 2 and positional parameters in Table 8. The ORTEP diagram is

Table 8 Positional parameters of complex **5a**

Atom	x	y	z
Pt	0	0	0
P(1)	0.136 2(2)	-0.057 24(9)	0.118 22(9)
P(2)	0.354 8(2)	-0.010 83(9)	0.270 6(1)
N	0.243 8(6)	0.007 9(3)	0.175 1(3)
N(1)	0.128 5(6)	0.162 0(3)	0.061 9(4)
C(1)	0.078 0(6)	0.104 2(3)	0.036 8(4)
C(11)	0.269 4(7)	-0.131 8(3)	0.085 0(4)
C(12)	0.420 0(8)	-0.110 9(4)	0.068 1(4)
C(13)	0.517 0(9)	-0.168 8(5)	0.036 6(6)
C(14)	0.462(1)	-0.242 2(6)	0.021 7(6)
C(15)	0.314(1)	-0.260 9(5)	0.035 4(5)
C(16)	0.217 1(8)	-0.206 7(4)	0.067 9(5)
C(21)	0.013 4(6)	-0.108 2(3)	0.190 0(4)
C(22)	-0.145 7(7)	-0.094 2(4)	0.183 3(4)
C(23)	-0.239 8(8)	-0.132 3(4)	0.239 1(4)
C(24)	-0.174 7(8)	-0.183 2(4)	0.300 0(4)
C(25)	-0.017 3(8)	-0.196 4(4)	0.307 6(4)
C(26)	0.076 9(7)	-0.159 2(4)	0.252 5(4)
C(31)	0.267 0(7)	0.054 4(4)	0.346 4(4)
C(32)	0.222 7(9)	0.025 2(4)	0.423 9(5)
C(33)	0.155 3(9)	0.073 9(4)	0.483 7(5)
C(34)	0.135 0(8)	0.150 0(4)	0.464 8(5)
C(35)	0.176 5(8)	0.179 9(4)	0.388 9(5)
C(36)	0.240 7(8)	0.133 5(4)	0.329 9(4)
C(41)	0.530 9(7)	0.044 8(4)	0.254 6(4)
C(42)	0.562 9(9)	0.081 8(4)	0.179 4(5)
C(43)	0.704 5(9)	0.118 3(5)	0.170 8(5)
C(44)	0.817 3(9)	0.115 3(5)	0.239 4(5)
C(45)	0.786 8(9)	0.079 4(5)	0.313 0(5)
C(46)	0.645 7(8)	0.043 1(4)	0.322 6(5)

shown in Fig. 4, selected bond lengths and angles in Table 9. The *trans* configuration and the planarity of the PtP<sub>2</sub>C<sub>2</sub> coordination sphere are crystallographically imposed as the platinum centre sits on the centre of inversion of the crystal's P<sub>2</sub>/c space group.

The ligand adopts a conformation of quasi-C<sub>s</sub> symmetry in the solid state. Its P<sub>2</sub>N plane lies essentially coplanar with the PtP(CN) co-ordination plane (Fig. 5); the dihedral angle between these planes is  $5.9^{\circ}$ . The absence of significant intermolecular contacts (all non-hydrogen atom separators are  $>3.0$  Å) suggests that such factors are not significant in determining the C<sub>s</sub> conformation or coplanarity of the PtP(CN)

Table 9 Selected bond distances (Å) and angles ( $^{\circ}$ ) for complex **5a**

Pt-P(1)	2.314(1)	P(2)-N	1.727(5)
Pt-C(1)	1.981(6)	P(2)-C(31)	1.828(6)
P(1)-N	1.663(5)	P(2)-C(41)	1.829(6)
P(1)-C(11)	1.823(6)	N(1)-C(1)	1.140(7)
P(1)-C(21)	1.817(5)		
P(1)-Pt-C(1)	91.0(2)	C(11)-P(1)-C(21)	104.2(3)
Pt-P(1)-N	111.1(2)	N-P(2)-C(31)	101.7(3)
Pt-P(1)-C(11)	111.7(2)	N-P(2)-C(41)	101.5(3)
Pt-P(1)-C(21)	113.7(2)	C(31)-P(2)-C(41)	99.0(3)
N-P(1)-C(11)	106.5(3)	P(1)-N-P(2)	125.2(3)
N-P(1)-C(21)	109.3(2)	Pt-C(1)-N(1)	175.8(5)

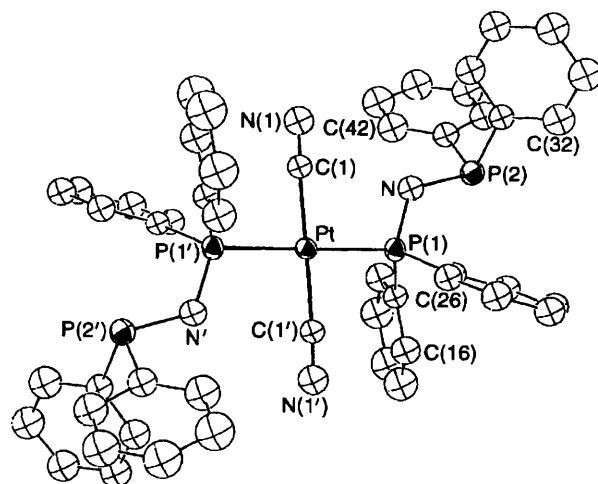


Fig. 4 An ORTEP diagram of [Pt(dppa-P)<sub>2</sub>(CN)<sub>2</sub>] **5a** showing the atom numbering scheme. Thermal ellipsoids represent 50% probability contours. Hydrogen atoms have been removed for clarity

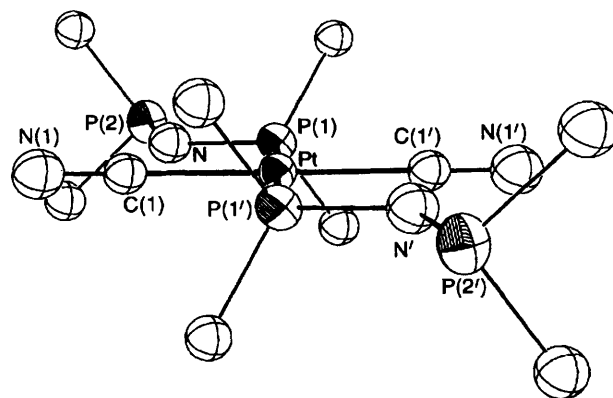


Fig. 5 An ORTEP diagram of complex **5a** illustrating the C<sub>s</sub> conformation of the ligand and the coplanarity of the P<sub>2</sub>N and PtP<sub>4</sub> planes. The phenyl rings, with the exception of their respective  $\alpha$ -C atoms, have been removed for clarity

and P<sub>2</sub>N planes. These features are absent in the crystal structure of *trans*-[Pd(dppm)<sub>2</sub>(Bu<sup>1</sup>NC)<sub>2</sub>].<sup>29</sup> The larger Bu<sup>1</sup>NC ligands may preclude the phosphine attaining such an orientation. The solid-state geometry of **5a** may be the product of a more efficient, compact packing of the complex in the lattice.

The P–N–P bond angle of 125.2(3)° is very close to that of 126.7° calculated for the ground-state H<sub>2</sub>PN(H)PH<sub>2</sub> structure of C<sub>s</sub> symmetry.<sup>10</sup> The P(1)–Pt–C(1) bond angle 91.0(2)° suggests that there is little steric crowding about the metal centre. The angles between the substituents of the co-ordinated phosphorus atom being significantly (> 10σ) greater than the corresponding angles within the unco-ordinated phosphino group is a well established feature of phosphine co-ordination chemistry.<sup>29</sup> The average N–P–C bond angle of 101.6(4)° between the phenyl and amino substituents of the unco-ordinated phosphorus atom is similar to that of 103.1(1)° observed in the free amine.<sup>18</sup> The Pt–P bond length of 2.314(1) Å is significantly (3.9σ) greater than the 2.298(4) Å average Pt–P bond distance observed in **3**.

Although the P–C<sub>phenyl</sub> bond distances of the co-ordinated end of the ligand are indistinguishable from those of the unco-ordinated end (or of the free amine<sup>18</sup>) both of the P–N bonds of the ligand are significantly different (5.4σ) from that of the free amine. The co-ordinated P(1)–N bond is 0.029(5) Å shorter and the P(2)–N bond is 0.035(5) Å longer than that of dppa.<sup>18</sup> The methylene C–P bond lengths of the dppm ligands in the solid-state structure of *trans*-[Pd(dppm)<sub>2</sub>(Bu<sup>1</sup>NC)<sub>2</sub>] qualitatively exhibit the same behaviour<sup>29</sup> as that of the P–N bonds of complex **5a**.

**Synthesis and Characterisation of the Dimeric Complex [Pt<sub>2</sub>(μ-dppa)<sub>2</sub>(CN)<sub>2</sub>] 6a.**—Upon demonstrating that dppa is a more effective chelator of Pt<sup>II</sup> than is dppm, it became of interest to determine its ability to bridge platinum centres as observed<sup>30</sup> with dppm in the formation of the platinum(I) dimeric complexes [Pt<sub>2</sub>(μ-dppm)<sub>2</sub>X<sub>2</sub>] (X = Cl, Br or I). Addition of 1 equivalent of [Pt(cod)<sub>2</sub>] to a solution of **5a** provided the platinum(I) dimer [Pt<sub>2</sub>(μ-dppa)<sub>2</sub>(CN)<sub>2</sub>] **6a**. The identity of the product was established by IR spectroscopy [ $\nu(\text{C}\equiv\text{N})$  2110 cm<sup>-1</sup> in CH<sub>2</sub>Cl<sub>2</sub>], mass spectrometry (Table 1), elemental analysis and <sup>31</sup>P-<sup>1</sup>H NMR spectroscopy. As the structure of **6a** gives rise to an A<sub>4</sub>/AA'A'A''X/AA'A'A''XX' spin system, spectral simulation<sup>31</sup> following the method of Brown *et al.*<sup>30</sup> provided the desired coupling constant data (Table 1). The similarity in the values calculated for **6a** with those of the related dppm complexes<sup>30</sup> suggests that **6a** has the structure shown in Scheme 1.

## Conclusion

The crystallographic characterisation of a number of structurally similar dpa chelate complexes of Pt<sup>II</sup> has permitted an evaluation of the nature of the ring strain in these systems. The bidentate compound bis(diphenylphosphino)amine (dppa) and its methyl derivative form stable chelate complexes with platinum despite the strain caused by the formation of the four-membered chelate ring. The small bite angle of the ligand compresses the P–N–P angle to approximately 100° which is a severe distortion from the ideal trigonal-planar angle expected at the sp<sup>2</sup>-hybridised nitrogen centre. Ring strain is evident structurally in the pyramidal character assumed at the nitrogen centres upon chelation. The crystallographic data also support a bent Pt–P bond as an effective model of the interaction between the platinum and phosphorus centres in the chelate complexes. The complexes are chemically and spectroscopically distinct from their dppm analogues. It is thought that the greater stability of the Pt<sup>II</sup>–dpa complexes, with respect to those of dppm, is the result of a more favourable metal–ligand interaction.

## Experimental

All reactions were performed in air, except where stated. For reactions which proved to be water-sensitive the solvents were

dried using standard techniques<sup>32</sup> and, for preparations involving the use of oxygen-sensitive materials, dissolved O<sub>2</sub> was excluded from the solvents by the freeze-evacuation method. Reactions requiring the exclusion of O<sub>2</sub> and/or water were carried out in an inert atmosphere of N<sub>2</sub>.

The <sup>31</sup>P NMR spectra were recorded on a Varian XL-200 spectrometer operating at 81.0 MHz or a Gemini 300 spectrometer at 121.5 MHz. The <sup>31</sup>P-<sup>1</sup>H NMR chemical shifts were measured with reference to external P(OMe)<sub>3</sub> in C<sub>6</sub>D<sub>6</sub> or CO(CD<sub>3</sub>)<sub>2</sub> and are reported with reference to 85% H<sub>3</sub>PO<sub>4</sub>. Infrared spectra of the complexes were recorded on a Nicolet 5DX FT-IR spectrometer in CH<sub>2</sub>Cl<sub>2</sub> solvent with the use of solution cells or as hydrocarbon mulls on NaCl plates. Fast-atom bombardment (FAB) mass spectrometric analyses were performed in a 3-nitrobenzyl alcohol matrix using a Varian VG70-250S mass spectrometer with a xenon gas ionising source at 8 kV and 1 mA. Chemical analyses were obtained from Chemical Microanalytical Service, New Westminster, B.C.

Deuterated solvents were obtained from MSD Isotopes. Other solvents and common reagents were from Aldrich, BDH, Digital or Fischer. The K<sub>2</sub>[PtCl<sub>4</sub>] starting material was from Strem Chemicals. The complexes [Pt(cod)Cl<sub>2</sub>], [Pt(cod)I<sub>2</sub>] and [Pt(cod)<sub>2</sub>] were synthesised using the technique of Whitesides and co-workers,<sup>33</sup> Drew and Doyle<sup>34</sup> and Spencer<sup>35</sup> respectively. Bis(diphenylphosphino)amine and bis(diphenylphosphino)methylamine were prepared following the method of Wang *et al.*<sup>36</sup>

**[Bis(diphenylphosphino)amine]dichloroplatinum(II) 1a.**—The compound dppa (482 mg, 1.25 mmol), dissolved in CH<sub>2</sub>Cl<sub>2</sub> (25 cm<sup>3</sup>) was added to a CH<sub>2</sub>Cl<sub>2</sub> solution (15 cm<sup>3</sup>) of [Pt(cod)Cl<sub>2</sub>] (1.25 mmol) over a period of 10 min. The product immediately precipitated as a colourless solid. The mixture was stirred for 1 h upon completion of the addition. The solid product was filtered off and washed with Et<sub>2</sub>O (5–10 cm<sup>3</sup>). Yield: >95%.

**[Bis(diphenylphosphino)methylamine]dichloroplatinum(II) 1b.**—An acetone solution (25 cm<sup>3</sup>) of dppma (500 mg, 1.25 mmol) was added to a solution of [Pt(cod)Cl<sub>2</sub>] (469 mg, 1.25 mmol) dissolved in CH<sub>2</sub>Cl<sub>2</sub> (15 cm<sup>3</sup>) over a period of 10 min. Precipitation of the colourless product occurred during the addition process. After the addition was complete the mixture was stirred for 1 h. Isolation by vacuum filtration and washing with cold Et<sub>2</sub>O (10 cm<sup>3</sup>) provided the product in 90% yield.

**[Bis(diphenylphosphino)amine]dicyanoplatinum(II) 2a.**—A solution of dppa (78 mg, 0.20 mmol) in CH<sub>2</sub>Cl<sub>2</sub> (10 cm<sup>3</sup>) was added in a rapid dropwise manner to [Pt(cod)I<sub>2</sub>] (112 mg, 0.20 mmol) dissolved in CH<sub>2</sub>Cl<sub>2</sub> (10 cm<sup>3</sup>). Reaction was not immediately evident as the solution maintained the original yellow colour of the [Pt(cod)I<sub>2</sub>] starting material. Precipitation of the intermediate complex [Pt(dppa)I<sub>2</sub>] occurred after stirring for 15 min. The solvent was removed under reduced pressure and the resultant pale yellow product was washed twice with aliquots (5 cm<sup>3</sup>) of CH<sub>2</sub>Cl<sub>2</sub>. Potassium cyanide (10 mg, 0.20 mmol) in MeOH (3 cm<sup>3</sup>) was added to a solution of the above product (83 mg, 0.10 mmol) dissolved in a minimum volume of Me<sub>2</sub>SO. The original yellow solution turned colourless over a period of 3 h. The complex [Pt(dppa)(CN)<sub>2</sub>] was selectively precipitated from solution as a white solid by the addition of methanol (20 cm<sup>3</sup>). Isolation by vacuum filtration and washing with MeOH (5 cm<sup>3</sup>) followed by acetone (5 cm<sup>3</sup>) gave the product in 70% yield [Found (Calc.): C, 49.4 (48.5); H 3.3 (3.2); N 6.6 (6.7)%].

**[Bis(diphenylphosphino)methylamine]dicyanoplatinum(II) 2b.**—Complex **1b** (133 mg, 0.200 mmol) was suspended in CH<sub>2</sub>Cl<sub>2</sub>–MeOH (1 : 1, 10 cm<sup>3</sup>). Sodium cyanide (20 mg, 0.408 mmol) was added as a solid with MeOH (2 cm<sup>3</sup>). After 15 min of stirring the NaCN had dissolved entirely while the solution remained clear



and colourless. The solvent was removed to dryness under reduced pressure. The addition of  $\text{CH}_2\text{Cl}_2$  ( $30\text{ cm}^3$ ) to the solid gave a solution of the desired product from which the small quantity of insoluble  $\text{NaCl}$  by-product was separated by filtration. Slow removal of the solvent under reduced pressure afforded the product as a microcrystalline white solid in  $>90\%$  yield.

**Chloride, Iodide and Tetrafluoroborate Salts of Bis[bis(diphenylphosphino)amine]platinum(II) 3a.**—**Chloride.** Slow dropwise addition of a solution of  $[\text{Pt}(\text{cod})\text{Cl}_2]$  (187 mg, 0.500 mmol) in  $\text{CH}_2\text{Cl}_2$  ( $25\text{ cm}^3$ ) to a solution of dppa (386 mg, 1.00 mmol) in  $\text{CH}_2\text{Cl}_2$ -MeOH (1:1,  $40\text{ cm}^3$ ) over a period of 10 min resulted in the precipitation of a white solid from a pale yellow solution. After stirring for 20 min, the solvent volume was reduced to approximately  $5\text{ cm}^3$ . The product mixture of  $[\text{Pt}(\text{dppa})_2\text{Cl}_2]$  and  $[\text{Pt}(\text{dppa})\text{Cl}_2]$  **1a** was filtered off and washed with  $\text{Et}_2\text{O}$  ( $5\text{ cm}^3$ ). The small quantity of insoluble **1a** by-product was removed by filtering the cloudy pale yellow solution obtained by redissolving the  $[\text{Pt}(\text{dppa})_2\text{Cl}_2]$  product in the minimum volume of  $\text{CH}_2\text{Cl}_2$ . Following the addition of MeOH ( $10\text{ cm}^3$ ), concentration of the solution to approximately  $5\text{ cm}^3$  afforded complex **3a** as the colourless microcrystalline chloride salt. It was filtered off and washed with  $\text{Et}_2\text{O}$  ( $10\text{ cm}^3$ ). Yield: 90%.

**Iodide.** The same procedure as that for the preparation of the chloride salt was used with  $[\text{Pt}(\text{cod})\text{I}_2]$  (278 mg, 0.500 mmol) and dppa (385 mg, 1.00 mmol) as reagents. Precipitation of the product occurred upon concentration of the yellow solution. The pale yellow solid was obtained in greater than 90% yield.

**Tetrafluoroborate.** The complex  $[\text{Pt}(\text{cod})\text{Cl}_2]$  (935 mg, 2.50 mmol) dissolved in the minimum volume of  $\text{CH}_2\text{Cl}_2$  was added in a rapid dropwise manner to a solution of dppa (1.93 g, 5.00 mmol) and  $\text{NaBF}_4$  (549 mg, 5.00 mmol) dissolved in the minimum volume of  $\text{CH}_2\text{Cl}_2$ -MeOH (1:1). In contrast to that of the above halide salts, the solution remains colourless throughout the addition. After stirring for 15 min, the solvent was removed to dryness under reduced pressure. Dichloromethane was added until no further dissolution of solid was evident. The resulting heterogeneous mixture was filtered to remove the insoluble  $\text{NaCl}$  by-product. The colourless solid product was precipitated upon addition of MeOH ( $10\text{ cm}^3$ ) followed by a reduction in solvent volume under reduced pressure. The compound was isolated by vacuum filtration and washed with  $\text{Et}_2\text{O}$  ( $10$ – $15\text{ cm}^3$ ). The absence of extraneous chloride in the product was confirmed by the lack of precipitation upon the addition of a small quantity of  $\text{Ag}(\text{O}_2\text{CMe})$  in MeOH. Yield: 90%.

The metathesised tetrafluoroborate salt of complex **3a** could also be prepared by a similar work-up of the solution obtained from the addition of the stoichiometric quantity of  $\text{NaBF}_4$  dissolved in a minimum volume of MeOH to a  $\text{CH}_2\text{Cl}_2$  solution of the chloride salt of **3a**.

$^{31}\text{P}$ - $\{^1\text{H}\}$  NMR spectroscopy was used to verify the *in situ* recovery of the tetrafluoroborate salt of complex **3a** as the product of the addition of several drops of 85%  $\text{HBF}_4$  in  $\text{Et}_2\text{O}$  to a  $\text{CH}_2\text{Cl}_2$  solution of **4**.

**Chloride, Iodide and Tetrafluoroborate Salts of Bis[bis(diphenylphosphino)methylamine]platinum(II) 3b.**—**Chloride.** The complex  $[\text{Pt}(\text{cod})\text{Cl}_2]$  (935 mg, 2.50 mmol) dissolved in the minimum volume of  $\text{CH}_2\text{Cl}_2$  was added in a rapid dropwise manner to a solution of dppma (2.00 g, 5.00 mmol) dissolved in the minimum volume of  $\text{CH}_2\text{Cl}_2$  to produce a yellow solution. After stirring for 10 min, the solution was filtered to remove insoluble impurities. The solvent volume was reduced to approximately  $30\text{ cm}^3$  under reduced pressure. Dropwise addition of  $\text{Et}_2\text{O}$  until the onset of precipitation produced large quantities of a pale yellow solid. Further precipitation was prompted by the addition of more  $\text{Et}_2\text{O}$  ( $10\text{ cm}^3$ ). Filtration and washing with  $\text{Et}_2\text{O}$  ( $15\text{ cm}^3$ ) provided the chloride salt as

a pale yellow microcrystalline solid which, upon standing for several minutes, underwent solvent loss to yield a colourless solid. Yield:  $>90\%$ .

**Iodide.** The same procedure as that for the chloride salt was used with  $[\text{Pt}(\text{cod})\text{I}_2]$  (1.393 g, 2.500 mmol) and dppma (1.997 g, 5.000 mmol) as reagents to yield a yellow-orange solution from which a yellow-orange microcrystalline solid was isolated. Standing in air caused it to become pale yellow as a result of solvent loss. Yield:  $>90\%$ .

The iodide salt was also generated *in situ*, characterised by  $^{31}\text{P}$ - $\{^1\text{H}\}$  NMR spectroscopy, by the addition of a stoichiometric excess of MeI to a  $\text{CH}_2\text{Cl}_2$  solution of complex **4** ( $48\text{ mg}$ ,  $5.0 \times 10^{-2}$  mmol). It could also be obtained by the dissolution of **4** in neat MeI.

**Tetrafluoroborate.** The complex  $[\text{Pt}(\text{cod})\text{Cl}_2]$  (935 mg, 2.50 mmol) dissolved in the minimum volume of  $\text{CH}_2\text{Cl}_2$  was added in a rapid dropwise manner to a solution of dppma (2.00 g, 5.00 mmol) and  $\text{NaBF}_4$  (549 mg, 5.00 mmol) dissolved in the minimum volume of  $\text{CH}_2\text{Cl}_2$ -MeOH (1:1). In contrast to that of the above halide salts, the solution remains colourless throughout the addition. After stirring for 15 min, the solvent was removed under reduced pressure. Dichloromethane was added until no further dissolution of solid was evident. The resulting heterogeneous mixture was filtered to remove the insoluble  $\text{NaCl}$  by-product. A colourless solid was precipitated by the addition of MeOH ( $10\text{ cm}^3$ ) followed by a reduction in solvent volume under reduced pressure. The compound was isolated by vacuum filtration and washed with  $\text{Et}_2\text{O}$  ( $15\text{ cm}^3$ ). The absence of extraneous chloride was confirmed by the lack of precipitation upon addition of a small quantity of  $\text{Ag}(\text{O}_2\text{CMe})$  in MeOH. Yield: 80%.

**Bis[bis(diphenylphosphino)amido]platinum(II) 4.**—A solution of  $[\text{Pt}(\text{dppa})_2(\text{BF}_4)_2]$  (285 mg, 0.250 mmol) in dry dmf ( $10\text{ cm}^3$ ) was added in a rapid dropwise manner to a dry dmf solution ( $3\text{ cm}^3$ ) of  $\text{LiNET}_2$  (20 mg, 0.25 mmol) under an inert atmosphere. Reaction was evident by the precipitation of a pale white solid approximately halfway through the addition. The mixture was stirred for 20 min and the product filtered off in air. After washing with MeOH ( $5\text{ cm}^3$ ) and thf ( $5\text{ cm}^3$ ), it was obtained in 85% yield [Found (Calc.): C, 58.8 (59.8); H, 4.4 (4.2); N, 3.0 (2.9)%].

**trans-Bis[bis(diphenylphosphino)amine-P]dicyanoplatinum(II) 5a.**—The slow addition of  $\text{NaCN}$  (12 mg, 0.25 mmol) in MeOH ( $10\text{ cm}^3$ ) to a solution of  $[\text{Pt}(\text{dppa})_2(\text{BF}_4)_2]$  (142 mg, 0.125 mmol) in a solvent mixture of MeOH ( $5\text{ cm}^3$ )- $\text{CH}_2\text{Cl}_2$  ( $10\text{ cm}^3$ ) over a period of 5 min resulted in precipitation of complex **5a** as a fine white solid. After the resultant mixture was stirred for 10 min, the solvent was removed under reduced pressure. Dichloromethane was added until no further dissolution of solid was evident. The resulting heterogeneous mixture was filtered to remove the insoluble  $\text{NaCl}$  by-product. A colourless solid was precipitated by the addition of MeOH ( $10\text{ cm}^3$ ) followed by a reduction in solvent volume under reduced pressure. It was filtered off and washed with MeOH ( $2\text{ cm}^3$ ) and thf ( $5\text{ cm}^3$ ). Yield: 75%.

**Bis[ $\mu$ -bis(diphenylphosphino)amine]dicyanodiplatinum(I) 6a.**—The complex  $[\text{Pt}(\text{cod})_2]$  (103 mg, 0.250 mmol) was added to the frozen surface of a dry  $\text{CH}_2\text{Cl}_2$  solution ( $25\text{ cm}^3$ ) of complex **5a** (254 mg, 0.250 mmol) under a nitrogen purge. The solution turned yellow upon slowly warming to room temperature and stirring for 15 min. A pale yellow solid precipitated upon slow addition of cold  $\text{Et}_2\text{O}$  ( $15\text{ cm}^3$ ) to the solution which had been reduced in volume to approximately  $5\text{ cm}^3$  under reduced pressure. The product **6a** was collected *via* vacuum filtration and washed with cold  $\text{Et}_2\text{O}$  ( $5\text{ cm}^3$ ). Yield: 70% [Found (Calc.): C, 47.8 (49.5); H, 3.8 (3.5); N, 4.5 (4.6)%].

**Competition Study between Bis(diphenylphosphino)amine and Bis(diphenylphosphino)methane.**—In order to determine the



relative stabilities of the dppm and dppa chelates of Pt<sup>II</sup> a solution of [Pt(cod)Cl<sub>2</sub>] (46 mg, 0.12 mmol) in CH<sub>2</sub>Cl<sub>2</sub> (10 cm<sup>3</sup>) was added to CH<sub>2</sub>Cl<sub>2</sub> (25 cm<sup>3</sup>) in which equimolar (96 mg, 0.25 mmol) quantities of dppm and dppa were completely dissolved. Formation of the [Pt(dppa)<sub>2</sub>]<sup>2+</sup> chelate as the exclusive product was determined by <sup>31</sup>P-<sup>1</sup>H NMR spectroscopy. The chloride salt of [Pt(dppa)<sub>2</sub>]<sup>2+</sup> was confirmed spectroscopically as the thermodynamic rather than the kinetic product of the competition study by the displacement of the chelated ligands of a CH<sub>2</sub>Cl<sub>2</sub> sample of [Pt(dppm)<sub>2</sub>Cl<sub>2</sub>]<sup>2+</sup> upon the addition of 2 equivalents of dppa.

**Crystallography.**—The unit-cell dimensions and the integrated intensities of the reflections of all crystal structures were measured at 295 K using an Enraf–Nonius CAD-4F diffractometer with graphite-monochromated Mo-K $\alpha$  radiation ( $\lambda = 0.71073 \text{ \AA}$ ) using  $\omega$ - $2\theta$  scans with a scan width of  $(0.75 + 0.35 \tan \theta)^\circ$  in  $\omega$ . Calculations were carried out on a PDP 11/23 computer using SDP<sup>37</sup> and an Apollo DSP 10020 minisupercomputer using the SHELX 76<sup>38</sup> and 86<sup>39</sup> packages. Neutral atom scattering factors were as provided in the SDP and SHELX 76 programs.

[Pt(dppa)<sub>2</sub>][BF<sub>4</sub>]<sub>2</sub>·MeCN. Colourless crystals of the complex were grown from CH<sub>2</sub>Cl<sub>2</sub>–MeCN–MeOH solution by slow evaporation. Accurate cell dimensions and the crystal orientation matrix were determined by a least-squares treatment of the setting angles of 25 reflections in the range  $7 < \theta < 15^\circ$ . Intensities of reflections with indices  $h$  0–10,  $k$  –12 to 12,  $l$  –14 to 14 were measured. An anisotropic decay correction was applied to the data due to a 73.0% decrease in the intensities of three standard reflections measured approximately every 4 h of X-ray exposure. The reflections measured were corrected for Lorentz and polarisation effects. An empirical absorption correction was applied to the data based upon  $\psi$  scans of five reflections with  $\theta$  values in the range  $4$ – $12^\circ$ . The transmission factors ranged from 78.93 to 99.66%. Crystal faces were identified as {100}, {010}, {001}, {101} and  $\{101\}$ . 2321 Unique data with  $I > 3\sigma(I)$  were regarded as observed and used in the structure solution and refinement. The chosen space group  $P\bar{1}$  was confirmed by a successful structure solution.

The structure was solved by the heavy-atom method. Refinement was by full-matrix least-squares calculations, initially with isotropic and then with anisotropic thermal parameters for the Pt, P and F atoms. A difference map showed maxima in positions consistent with the expected locations of hydrogen atoms. In the final rounds of calculations the hydrogen atoms were positioned on geometric grounds and included (as riding atoms) in the structure-factor calculation. The final cycle of refinement of 177 variable parameters converged to unweighted  $R$  and weighted  $R' = [\sum w(|F_o| - |F_c|)^2 / \sum w F_o^2]^{1/2}$  agreement factors to values of 0.042 and 0.058 respectively where the non-Poisson weighting function,  $w$ , defined as  $4F_o^2 / [\sigma(F_o)^2 + (0.05 F_o^2)^2]$  was used to downweight intense reflections. The maximum parameter shift/e.s.d. in the final cycle of refinement was 0.01; the highest peak in the final Fourier-difference map had an electron density of  $1.81 \text{ e \AA}^{-3}$  at position (0.139, 0.000, –0.021) which is associated with the Pt atom. No correction for secondary extinction was applied.

[Pt(dppma)<sub>2</sub>][BF<sub>4</sub>]<sub>2</sub>. Colourless crystals were grown from a CH<sub>2</sub>Cl<sub>2</sub>–Et<sub>2</sub>O solution of the complex by slow evaporation. Accurate cell dimensions and the crystal orientation matrix were determined as before. Intensities of reflections with indices  $h$  0–14,  $k$  0–21,  $l$  –19 to 19 were measured. The intensities of three standard reflections were measured as before and an anisotropic decay correction was applied due to a 2.2% decrease in intensity. The space group  $P2_1/n$  was determined by the systematic absences ( $0k0$  absent if  $k = 2n + 1$ ,  $h0l$  absent if  $h + l = 2n + 1$ ). The reflections measured were corrected for Lorentz and polarisation effects. An empirical absorption correction was applied based upon  $\psi$  scans of six reflections with  $\theta$  values in the range  $7$ – $15^\circ$ . The transmission factors

ranged from 66.55 to 99.94%. The equivalent reflections were averaged with  $R = 0.022$ . Crystal faces were identified as {011} and {101}. 3651 Unique data with  $I > 3\sigma(I)$  were regarded as observed and used in the structure solution and refinement.

The structure was solved and refined as for complex 3a. The final cycle of refinement of 169 variable parameters converged to  $R = 0.036$  and  $R' = 0.045$  respectively with the same weighting function as for 3a. The maximum parameter shift/e.s.d. in the final cycle of refinement was 0.01; the highest peak in the final Fourier-difference map had an electron density of  $1.06 \text{ e \AA}^{-3}$  at position (–0.057, 0.000, 0.020) which is associated with the Pt atom. No correction for secondary extinction was applied.

*trans*-[Pt(dppa-*P*)<sub>2</sub>(CN)<sub>2</sub>] 5a. Colourless crystals of complex 5a were grown from a CH<sub>2</sub>Cl<sub>2</sub>–MeOH solution by slow evaporation. Accurate cell dimensions and the crystal orientation matrix were determined by a least-squares treatment of the setting angles of 25 reflections in the range  $10 < \theta < 13^\circ$ . Intensities of reflections with indices  $h$  0–10,  $k$  0–20,  $l$  –20 to 20 were measured. The intensities of two reflections measured as before showed a decrease in intensity of less than 1%. The space group  $P2_1/c$  was determined by the systematic absences ( $0k0$  absent if  $k = 2n + 1$ ,  $h0l$  absent if  $l = 2n + 1$ ). The 4298 reflections measured were corrected for Lorentz and polarisation effects. Application of a gaussian absorption correction to the data gave transmission factors ranging from 71.55 to 77.28%. The equivalent reflections were averaged with  $R = 0.015$ . Crystal faces were identified as {100} and {011}. 2639 Unique data with  $I > 3\sigma(I)$  were regarded as observed and used in the structure solution and refinement.

The structure was solved and refined as before. The final cycle of refinement of 133 variable parameters converged to  $R = 0.030$  and  $R' = 0.040$  respectively with the same weighting function as for complex 3a. The maximum parameter shift/e.s.d. in the final cycle of refinement was 0.02; the highest peak in the final Fourier-difference map had an electron density of  $0.83 \text{ e \AA}^{-3}$  at position (0.500, –0.201, –0.021) which is associated with C(13). No correction for secondary extinction was applied.

Additional material available from the Cambridge Crystallographic Data Centre comprises H-atom coordinates, thermal parameters and remaining bond lengths and angles.

## Acknowledgements

We thank Dr. Alex Young for the mass spectra. Funding provided by the Natural Sciences and Engineering Research Council of Canada is also gratefully acknowledged.

## References

- 1 S. S. M. Ling, R. J. Puddephatt, L. Manojlović-Muir and K. W. Muir, *Inorg. Chim. Acta*, 1983, **77**, L95.
- 2 A. R. Langer, *J. Chem. Soc., Dalton Trans.*, 1977, 1971.
- 3 F. S. M. Hassan, D. P. Markham, P. G. Pringle and B. L. Shaw, *J. Chem. Soc., Dalton Trans.*, 1985, 279; P. G. Pringle and B. L. Shaw, *J. Chem. Soc., Chem. Commun.*, 1982, 956.
- 4 I. M. Al-Najjar, *Inorg. Chim. Acta*, 1987, **128**, 93.
- 5 P. S. Braterman, R. J. Cross, L. Manojlović-Muir, K. W. Muir and G. B. Young, *J. Organomet. Chem.*, 1975, **84**, C40.
- 6 F. S. M. Hassan, D. M. McEwan, P. G. Pringle and B. L. Shaw, *J. Chem. Soc., Dalton Trans.*, 1985, 1501.
- 7 T. G. Appleton, M. A. Bennett and I. B. Tomkins, *J. Chem. Soc., Dalton Trans.*, 1976, 439.
- 8 S. Hietkamp, D. J. Stufkens and K. Vrieze, *J. Organomet. Chem.*, 1979, **169**, 107.
- 9 (a) R. Usón, J. Forníes, R. Navarro and J. I. Cebollada, *J. Organomet. Chem.*, 1986, **304**, 381; (b) R. Usón, J. Forníes, P. Espinet, R. Navarro and C. Fortuño, *J. Chem. Soc., Dalton Trans.*, 1987, 2077.
- 10 C. S. Browning, D. H. Farrar and M. R. Peterson, *J. Mol. Struct.*, 1991, **251**, 153.

- 11 C. S. Browning, D. H. Farrar and D. C. Frankel, *Acta Crystallogr., Sect. C*, 1992, **48**, 806.
- 12 M. S. Balakrishna, V. Sreenivasa Reddy, S. S. Krishnamurthy, J. F. Nixon and J. C. T. R. Burckett St. Laurent, *Coord. Chem. Rev.*, 1994, **129**, 1.
- 13 S. Vianello, M. Bonivento, L. Cattalini, O. Curcuruto and P. Traldi, *Rapid Commun. Mass Spectrom.*, 1991, **5**, 479.
- 14 C. S. Browning and D. H. Farrar, unpublished work.
- 15 C. K. Johnson, ORTEP, Report ORNL-5138, Oak Ridge National Laboratory, Oak Ridge, TN, 1976.
- 16 G. Liehr, G. Szucsányi and J. Ellerman, *J. Organomet. Chem.*, 1984, **265**, 95.
- 17 T. G. Appleton, H. C. Clark and L. E. Manzer, *Coord. Chem. Rev.*, 1973, **10**, 335 and refs. therein.
- 18 H. Nöth and E. Fluck, *Z. Naturforsch., Teil B*, 1984, **39**, 744.
- 19 F. H. Allen, O. Kennard, D. G. Watson, L. Brammer, A. G. Orpen and R. Taylor, *J. Chem. Soc., Perkin Trans. 2*, 1987, S1.
- 20 H. C. Clark and M. J. Hampden-Smith, *Coord. Chem. Rev.*, 1987, **79**, 229.
- 21 C. A. Tolman, *Chem. Rev.*, 1977, **77**, 313.
- 22 Q.-B. Bao, S. J. Geib, A. L. Rheingold and T. B. Trill, *Inorg. Chem.*, 1987, **26**, 3453.
- 23 R. Keat, L. Manojlovic-Muir, K. W. Muir and D. S. Rycroft, *J. Chem. Soc., Dalton Trans.*, 1981, 2192.
- 24 J. A. A. Mokuolu, D. S. Payne and J. C. Speakman, *J. Chem. Soc., Dalton Trans.*, 1973, 1443.
- 25 M. C. Grossel, R. P. Moulding, K. R. Seddon and F. J. Walker, *J. Chem. Soc., Dalton Trans.*, 1987, 705.
- 26 G. G. Mather, A. Pidcock and G. J. N. Rapsey, *J. Chem. Soc., Dalton Trans.*, 1973, 2095; J. F. Nixon and A. Pidcock, *Annu. Rev. N.M.R. Spectrosc.*, 1969, **2**, 346.
- 27 J. Powell, *J. Chem. Soc., Chem. Commun.*, 1989, 200.
- 28 H. Schmidbauer, S. Lauteschläger and B. Milewski-Mahrla, *J. Organomet. Chem.*, 1983, **254**, 59.
- 29 M. M. Olmstead, Chung-Li Lee and A. L. Balch, *Inorg. Chem.*, 1982, **21**, 2712.
- 30 M. P. Brown, R. J. Puddephatt, M. Rashidi and K. R. Seddon, *J. Chem. Soc., Dalton Trans.*, 1977, 951.
- 31 L. Cassidei and O. Sciacovelli, locally modified version of Quantum Chemistry Program Exchange Program No. 458, LAOCN-5, Department of Chemistry, University of Bari, 1984.
- 32 D. F. Shriver and M. A. Drezdson, *The Manipulation of Air-sensitive Compounds*, 2nd edn., Wiley, New York, 1986.
- 33 J. X. McDermott, J. F. White and G. M. Whitesides, *J. Am. Chem. Soc.*, 1976, **98**, 6521.
- 34 D. Drew and J. R. Doyle, *Inorg. Synth.*, 1972, **13**, 50.
- 35 J. L. Spencer, *Inorg. Synth.*, 1979, **19**, 213.
- 36 F. T. Wang, J. Najdzionek, K. L. Leneker, H. Wasserman and D. M. Braitsch, *Synth. React. Inorg. Metal-Org. Chem.*, 1978, **8**, 119.
- 37 B. A. Frenz, SDP Structure Determination Package, College Station, TX and Enraf-Nonius, Delft, 1982.
- 38 G. M. Sheldrick, SHELX 76, Program for crystal structure determination and refinement, University of Cambridge, 1976.
- 39 G. M. Sheldrick, SHELX 86, Program for crystal structure determination, University of Göttingen, 1986.

Received 18th August 1994; Paper 4/05064I